Sustainable Food Technology

ROYAL SOCIETY OF CHEMISTRY

PAPER

View Article Online
View Journal

Cite this: DOI: 10.1039/d5fb00851d

Inulin's paradoxical effect on Ca(II)-alginate encapsulation of phenolic extracts

Peyman Ebrahimi, *[a] Alberto De Iseppi, [a] Zeynep Gülbeş,[a] Elisa Canazza, [a] Jacopo Nava, [b] Barbara Simonato, [c] Corrado Rizzi, [c] Dasha Mihaylova [d] and Anna Lante *[a]

Encapsulating polyphenols in Ca(II)-alginate beads requires suitable co-carriers, such as inulin, to reduce bead porosity and enhance protective efficiency. However, the real impact of inulin remains unknown, with some studies showing improved encapsulation efficiency (EE) and others indicating a decline. This study investigated the actual effect of inulin on the EE, physical properties, and release behaviour of Ca(II)-alginate beads loaded with spent sour cherry pomace extracts. EE based on total phenolic content (TPC) determined from bead dissolution in sodium citrate increased significantly with inulin addition, exceeding 90%. In contrast, TPC-based EE calculated from unloaded compounds in the residual calcium chloride solution decreased with inulin, dropping below 40%. This inconsistency was attributed to interference from inulin in the Folin–Ciocalteu assay, as its incorporation into the bead matrix may lead to overestimated TPC values. Supporting this, pure inulin exhibited a measurable TPC of 74.79 ± 2.28 μg GAE per g and notable reducing activity in the ferric-reducing antioxidant assay. Moreover, beads containing inulin exhibited reduced hardness, due to increased viscosity of the feed solution, which likely hindered alginate-calcium cross-linking. However, inulin significantly enhanced anthocyanin-based EE from 47.18 ± 2.54% to 53.26 ± 0.91% ($p \leq 0.05$). It also increased the beads' diameter, filling the pores within the Ca(II)-alginate matrix, as confirmed by SEM imaging. Release kinetics of TPC and anthocyanins followed the Korsmeyer–Peppas model ($R^2 > 0.9$), with n values indicating Fickian diffusion. Although inulin reduced apparent TPC-based EE and bead rigidity, its functional advantages warrant further optimization of formulation parameters.

Received 31st October 2025
Accepted 21st January 2026

DOI: 10.1039/d5fb00851d

rsc.li/susfoodtech

Sustainability spotlight

The increasing emphasis on sustainable food systems necessitates the valorization of agri-food by-products and the substitution of synthetic additives with natural alternatives. This study utilizes spent sour cherry pomace, a by-product of liqueur manufacturing, as a renewable source of polyphenols. Moreover, it develops a clean-label delivery system using inulin and alginate, which are both food-grade and biodegradable polysaccharides. The research addresses analytical challenges in measuring encapsulation efficiency and offers new perspectives on the design of environmentally friendly polysaccharide matrices for the stabilization and controlled release of natural antioxidants. This approach supports United Nations Sustainable Development Goals 12 (Responsible Consumption and Production) and 9 (Industry, Innovation, and Infrastructure) by promoting waste valorization and sustainable formulation strategies.

1 Introduction

The search for safe and effective natural antioxidants, particularly polyphenol-based compounds, has been a significant focus of research over the past few decades.[1] In this context, increasing attention has been directed toward extracting them from plant matrices, especially those regarded as food processing by-products. These underutilized materials represent cost-effective sources for the recovery of bioactive compounds.[2,3] For instance, spent sour cherry pomace (SSCP), which is a by-product of sour cherry liqueur production in Italy, is rich in phenolic compounds, particularly anthocyanins.[4] However, these compounds are highly sensitive to environmental factors such as oxygen, temperature, light, pH, transition metals, and

[a]Department of Agronomy, Food, Natural Resources, Animals, and Environment—DAFNAE, University of Padova, Viale dell'Università, 16, 35020 Legnaro, Italy. E-mail: anna.lante@unipd.it; peyman.ebrahimi@unipd.it; alberto.deiseppi@unipd.it; zeynep.guelbes@studenti.unipd.it; elisa.canazza.3@studenti.unipd.it

[b]Department of Geosciences, University of Padova, Via Giovanni Gradenigo 6, 35131 Padova, Italy. E-mail: Jacopo.nava@unipd.it

[c]Department of Biotechnology, Università Di Verona, Strada Le Grazie 15, Verona, 37134, Italy. E-mail: barbara.simonato@univr.it

[d]Department of Microbiology and Biotechnology, University of Food Technologies, 26 Maritza Blvd., 4002 Plovdiv, Bulgaria. E-mail: dashamihaylova@yahoo.com

enzymes.[5] Therefore, it is essential to develop encapsulation strategies that can protect the bioactive compounds of phenolic extracts from harsh environmental conditions.

Encapsulation of phenolic extracts can be performed using various techniques and wall materials, each offering distinct advantages and limitations.[6] Due to the health concerns arising from the use of synthetic wall materials, greater emphasis has been placed on the use of natural alternatives.[7] Alginate is a natural wall material isolated from brown algae, which is a polymer composed of D-mannuronic acid and L-guluronic acid linked by the α-1–4 glycosidic bond.[8,9] It exhibits unique colloidal properties and can form versatile, biocompatible, and food-grade Ca(II)-alginate hydrogels through cross-linking with calcium ions.[10] The ability of alginate to form hydrogels under mild conditions, without the use of organic solvents or elevated temperatures, makes it particularly suitable for encapsulating sensitive compounds such as polyphenols. However, Ca(II)-alginate beads often exhibit high surface porosity, allowing bioactive compounds to come into contact with oxygen.[11] Therefore, it is necessary to identify an appropriate co-carrier or filler to reduce the porosity of these beads and enhance their protective efficiency.

Inulin is a linear polydisperse polysaccharide consisting mainly of β-(2 $\rightarrow$ 1) fructosyl-fructose linkages.[12] It has potential applications in functional foods and pharmaceutical formulations as a dietary fiber with well-documented health benefits, including immune system modulation through stimulation of intestinal microflora.[13] In addition to its physiological effects, inulin exhibits valuable technological properties, serving as a bulking agent and stabilizer in various food systems. Owing to these characteristics, inulin may provide structural reinforcement to Ca(II)-alginate beads by acting as a pore-filling co-carrier.[12] While some studies have observed a positive correlation between inulin concentration and encapsulation efficiency (EE) in the ionic gelation method,[13] others have reported a decrease in efficiency when higher concentrations of inulin were used.[14] Building on these findings, the present study seeks to clarify the actual effect of inulin as a co-carrier in Ca(II)-alginate beads, determining whether its addition enhances or compromises encapsulation performance.

Both inulin and alginate possess a favorable regulatory status worldwide, being classified as Generally Recognized as Safe (GRAS) in the United States and approved by the European Food Safety Authority (EFSA) for food applications.[15,16] The use of aqueous SSCP extracts, inulin derived from chicory roots, and sodium alginate for bead preparation in this study aligns with a fully clean-label formulation strategy, promoting the use of natural ingredients. This approach supports the development of functional encapsulated products that meet consumer demand for safe, sustainable, and transparent food ingredients.

Although several studies have focused on encapsulating SSCPs derived from juice processing,[17,18] none have focused on encapsulating SSCP extracts obtained from residues of liquor production. In brief, the present work focuses on the encapsulation of these SSCP extracts while clarifying the actual effect of inulin as a co-carrier in Ca(II)-alginate beads. Specifically, the study aims to elucidate how the combination of inulin and alginate influences EE, bead physical characteristics, and the release behavior of phenolic compounds.

2 Experimental

2.1 Materials and chemicals

The SSCP samples were by-products of sour cherry liqueur production after the fermentation process of pitted sour cherries at a local distillery in Verona, Italy. The sour cherries (*Prunus cerasus* L. var. *Marasca*) used in the distillery were sourced from various regions based on the optimal ripeness of the fruit for each production batch. Food-grade inulin powder, derived from chicory roots (*Cichorium intybus*) and composed of $\geq$99% oligo- and polysaccharides with an average degree of polymerization ranging from 8 to 13 monomers, was obtained from Laboratori Bio Line Srl, Rovigo, Italy. All chemicals and solvents were of analytical grade, with purities over 98%. Sodium acetate, sodium alginate, acetic acid, hydrochloric acid, sodium carbonate, sodium hydroxide, calcium chloride, sodium citrate tribasic dehydrate, Folin–Ciocalteu reagent, iron(III) chloride, 2,4,6-tris(2-pyridyl)-*s*-triazine (TPTZ), potassium hydroxide, and potassium chloride were purchased from Sigma (St. Louis, MO, USA). Double-distilled water was used in all the analyses.

2.2 Extract preparation

The extraction of polyphenols was performed according to the optimum conditions reported by Ebrahimi *et al.* (2025)[4] with some minor modifications. First, the SSCPs were dried in a freeze-dryer (Modulyo, Edwards, West Sussex, UK) under 28 mbar at -50 °C for 4 days, and then ground into a fine powder using a mortar and pestle. Then, 0.4 g of the freeze-dried powder was added to 10 mL of water and vortexed for 30 s. The extraction was performed using an ultrasound apparatus (HD 2200.2, Bandelin, Berlin, Germany), equipped with a titanium probe model KE 76, at 200W power, 25% amplitude, 9 min time, and 20 kHz frequency. To prevent overheating and maintain the initial temperature (20 $\pm$ 2 °C), the sonication was performed in 60 second cycles with 10 second pauses in the middle, and the extraction cell was placed in an ice bucket throughout the process. After ultrasonication, the mixtures were centrifuged at 4 °C and 4000$\times g$ for 10 min. The supernatants were filtered using Whatman® no. 1 filter papers and stored at -80 °C until subsequent use.

2.3 Individual phenolic compounds of the extract

The individual phenolic compounds in the SSCP extract were quantified according to Ebrahimi *et al.* (2024).[19] An HPLC apparatus (1260 Infinity II Prime LC, Agilent, Santa Clara, CA, USA) equipped with a diode array detector (DAD) and a Poroshell 120 EC-C18 column (2.7 μm *i.d.*, 3.0 $\times$ 150 mm; Agilent, Santa Clara, CA, USA) was used to perform the test. The column and guard column were kept at a constant temperature of 30 °C. A 1.5 μL aliquot of either the extract or standard solution was injected for each run. The chromatographic separation was achieved using a mobile phase of Milli-Q water (solvent A) and acetonitrile (solvent B), both acidified with 0.1% formic acid, at a flow rate of 0.3 mL min^{-1}. The gradient program started with

15% B, increased to 40% over 40 min, and then from 40% to 100% B within 5 min. Between runs, the column was re-equilibrated with 100% A for 10 min. Detection of phenolic compounds was carried out at a wavelength of 280 nm. Standard stock solutions were prepared in ethanol, and calibration curves ($R^2 \geq 0.99$) for each phenolic standard were used to quantify compound concentrations, expressed in mg L^{-1}.

2.4 Encapsulation of the extract

The Ca(II)-alginate beads were prepared according to Dallabona *et al.* (2020),[20] with some modifications. Inulin was dissolved at different levels (0, 0.5, 1, 1.5, 2, and 3 g) in 10 g of the prepared extract, followed by the addition of 10 g of a 3% (w/w) sodium alginate solution. The resulting feed solutions contained 1.5% (w/w) sodium alginate, 50% (w/w) extract, and 0, 2.5, 5, 7.5, 10, or 15% (w/w) inulin, respectively. Each feed solution was dispensed dropwise (□2 drops per second) into 80 mL of 5% (w/v) calcium chloride, as a crosslinking solution, using a 5 mL syringe without a needle (Fig. 1). The suspensions were stirred for 10 minutes on a magnetic stirrer to allow complete bead formation. The hydrogel beads were then separated from the crosslinking solution using a Whatman® no. 1 filter, rinsed once with ultrapure water, and blotted on paper towels for 5 min to remove surface moisture. The residual calcium chloride solutions were used to determine the amount of unencapsulated compounds for calculating EE. A portion of the hydrogel beads was freeze-dried at −50 °C under 28 mbar for 4 days for SEM and release studies, while the rest was analyzed immediately.

2.5 Viscosity of the feed solution

The shear flow viscosity of the feed solutions used for bead preparation was measured according to Teslić *et al.* (2025)[21] with some modifications. Measurements were performed using a Kinexus Pro rheometer (Malvern Panalytical Ltd, Malvern, UK) equipped with a parallel plate geometry (60 mm diameter). For each analysis, 2 g of the feed solution was placed on the rheometer plate at 25 °C. The shear rate was varied from 0.01 to 1000 s^{-1}. Each test was conducted in triplicate, and the mean values were used to construct the viscosity-shear rate curve. The obtained data were fitted to the cross model to determine the zero-shear viscosity (η_0).

2.6 Detection of inulin

The residual calcium chloride solutions obtained after bead preparation were analyzed to determine the amount of unloaded inulin, which was used to calculate the EE, as described in Section 2.10. To do so, each solution was filtered through a 0.22 μm Millipore membrane before the experiment. The HPLC analysis was performed using a Jasco system (Jasco Corporation, Tokyo, Japan) equipped with an isocratic pump, a CO-2060 column oven maintained at 80 °C, and a RI-2031 Plus refractive index detector. Separation was achieved on an Aminex HPX-87C carbohydrate column (300 mm × 7.8 mm, Bio-Rad) under isocratic conditions, with ultrapure water (Type 1, 18.2 MΩ cm) as the mobile phase at a flow rate of 0.6 mL min^{-1}. Data acquisition and processing were performed using the ChromNAV software. Calibration curves were prepared using inulin standards in the concentration range of 0.01–20 mg mL^{-1}. Method accuracy and precision were verified with a blank, a low-level control (recovery limits ±30%), and a medium-level control (recovery limits ±10%).

2.7 Total phenolic content (TPC)

The TPC of the extract, the relevant solutions used for EE determination (Section 2.10), and inulin were analyzed using

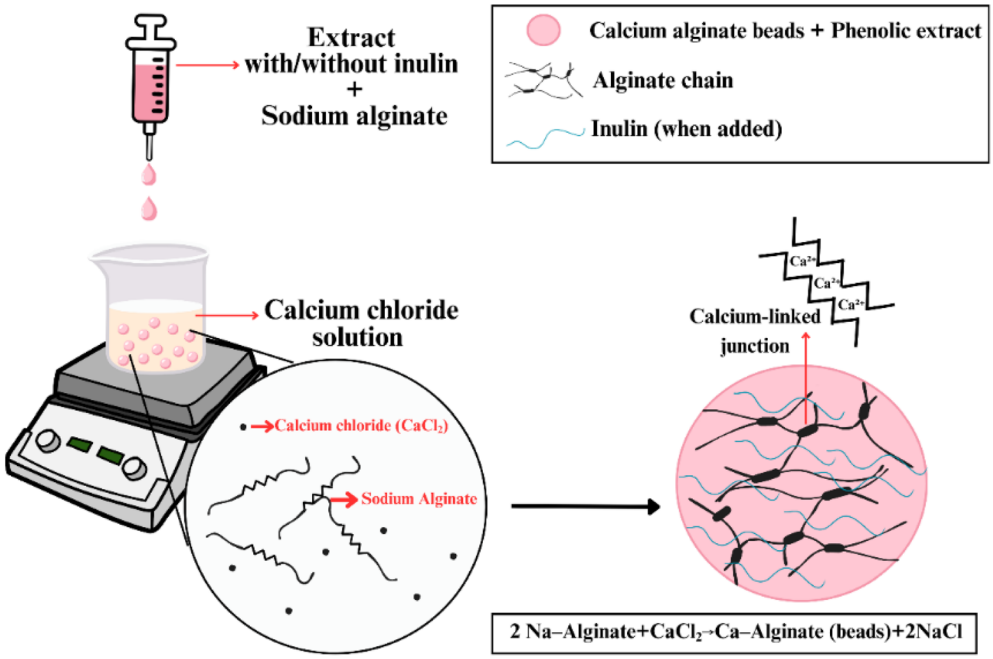

Fig. 1 Schematic of preparation of Ca(II)-alginate beads.

the Folin–Ciocalteu colorimetric method as described by Azuma *et al.* (1999).[22] Briefly, 200 μL of the sample was mixed with 1 mL of 10% (w/v) sodium carbonate (Na_2CO_3) in 1 M sodium hydroxide, and 100 μL of two-times diluted Folin–Ciocalteu reagent. For the blank sample, 200 μL of water was used instead of the sample. The mixtures were incubated at room temperature in the dark for 30 min. After centrifuging at 4 °C and 8000×*g* for 1 min, the absorbance of the mixture at 650 nm was measured using a spectrophotometer (Varian Carry 50 Bio UV/Vis, Agilent Technologies, Santa Clara, CA, USA). A standard curve of gallic acid ($R^2 \geq 0.99$) was used to report results as mg gallic acid equivalent per L of extract (mg GAE per L).

2.8 Total monomeric anthocyanin content (TMAC)

The TMAC of the extract and the relevant solutions used for EE determination (Section 2.10) was determined using the pH differential method as described by Dallabona *et al.* (2020),[20] with minor modifications. First, 500 μL of the sample was added to 1500 μL of 0.025 M potassium chloride buffer at pH 1.0 and 0.4 M sodium acetate buffer at pH 4.5. Similar mixtures were prepared using 500 μL of water instead of the sample as blanks. After a 15 minute incubation at room temperature, the absorbance of the mixtures was recorded at 520 and 700 nm. The TMAC was calculated using eqn (1).

$$\mathrm{TMAC}\left(\mathrm{mg\ L^{-1}}\right) = \frac{A \times \mathrm{MW} \times \mathrm{DF} \times 1000}{\varepsilon \times 1} \quad (1)$$

where $A = (A_{520\mathrm{nm}} - A_{700\ \mathrm{nm}})_{\mathrm{pH1}} - (A_{520\ \mathrm{nm}} - A_{700\mathrm{nm}})_{\mathrm{p4.5}}$, MW is the molecular weight (449.2 g $\mathrm{mol^{-1}}$), ε is the molar absorptivity of cyanidin-3-glucoside (26900 L $\mathrm{mol^{-1}}$ cm), and DF is the dilution factor, assuming a cell path length of 1 cm.

2.9 Determination of the antioxidant activity

Antioxidant activity of the extract and inulin was measured using the ferric reducing antioxidant power (FRAP) method as described by Zhou *et al.* (2017)[23] with minor modifications. First, the FRAP reagent was prepared by mixing 25 mL of 30 mM sodium acetate buffer (pH 3.6), 2.5 mL of 20 mM iron(III) chloride, and 2.5 mL of 10 mM TPTZ dissolved in 40 mM HCl. Next, 100 μL of the sample was added to 900 μL of FRAP reagent, and for the blank sample, 100 μL of water was used instead of the sample. All the mixtures were incubated at 37 °C for 30 min, and the absorbance was recorded at 593 nm. A standard curve of Trolox ($R^2 \geq 0.99$) was used to express the results as mg Trolox equivalent per L of extract (mg TE per L).

2.10 Encapsulation efficiency (EE) and process yield

The EE of the extract in the beads was determined as described by Dallabona *et al.* (2020).[20] Two complementary approaches were used to provide a more accurate understanding of the encapsulation behavior as described below.

The first method (EE based on unloaded compounds) provides an estimation of the actual encapsulated fraction by accounting for the non-entrapped components remaining in the residual $CaCl_2$ solution. In this case, the inulin content, TPC, and TMAC in the $CaCl_2$ solution were analyzed using the methods described in Sections 2.6, 2.7, and 2.8, respectively. The EE based on unloaded compounds (%) was calculated using eqn (2).

$$\text{EE based on unloaded compounds } (\%) = \frac{M_0 - M_u}{M_0} \times 100 \quad (2)$$

where M_0 is the total mass of compounds initially present in the extract (mg), and M_u is the mass of unloaded (non-encapsulated) compounds detected in the residual $CaCl_2$ solution (mg).

The second method (EE based on loaded compounds) was included for comparative purposes, as it is commonly used in the literature. In this approach, 0.1 g of freeze-dried beads was completely dissolved in 5 mL of 5% (w/v) sodium citrate solution at 100 rpm for 2 h, and the resulting solution was used to quantify the loaded fraction. The EE based on loaded compounds (%) was then calculated according to eqn (3).

$$\text{EE based on loaded compounds } (\%) = \frac{M_l}{M_0} \times 100 \quad (3)$$

where M_l is the mass of loaded compounds in the beads (mg), and M_0 is the mass of compounds initially present in the extract (mg).

The process yield was calculated as the ratio of the total mass of obtained beads to the total mass of the feed solution (*i.e.,* the mixture of the extract, sodium alginate, and inulin). The process yield is expressed as a percentage, as shown in eqn (4).

$$\text{Process Yield } (\%) = \frac{W_b}{W_f} \times 100 \quad (4)$$

where W_b is the total mass of the obtained beads (g), and W_f is the total mass of the feed solution (g), consisting of the extract, sodium alginate, and inulin.

2.11 Determination of hygroscopicity, moisture, and water activity of beads

Hygroscopicity was evaluated according to Pattnaik and Mishra (2020).[24] Briefly, 0.1 g of freeze-dried beads was placed in Petri dishes and stored in a glass desiccator containing a saturated NaCl solution (75.6% relative humidity) at 25 ± 1 °C. After 7 days, the samples were reweighed, and hygroscopicity was calculated using eqn (5). The moisture content was determined using the oven-drying method at 105 °C for 24 h. Water activity (a_w) was measured at 25 °C using a LabMaster-aw instrument (Novasina AG, Lachen, Switzerland).

$$\text{Hygroscopicity } (\%) = \frac{W_1 - W_0}{W_1} \times 100 \quad (5)$$

where W_1 is the weight of the beads after 7 days, and W_0 is the initial weight of the beads (day 0).

2.12 Determination of the mechanical properties of the beads

The texture of the hydrogel beads was analyzed using a TA.XT-plus Texture Analyzer (Stable Micro Systems, Surrey, UK) equipped with a 20 mm diameter compression probe. Plastic Petri dishes were filled with beads (diameter: 35 mm, height: 11

mm; Thermo Fisher Scientific, Waltham, MA, USA) during testing. The texture of the beads was tested at room temperature with a compression speed of 0.5 mm s^{-1}, and a deformation of 50% of the bead height. A load cell capacity of 50 N and a data acquisition rate of 250 points per second were used. The resulting curves were analyzed to determine hardness, springiness, cohesiveness, elasticity index, gumminess, and resilience. Each parameter was calculated based on the specific regions and peaks identified in the force–time curves. The beads' diameters were measured using a Vernier caliper.

2.13 Scanning electron microscopy (SEM)

The freeze-dried beads were examined using scanning electron microscopy (SEM) based on the secondary electron (SE) imaging mode. Prior to imaging, the samples were coated with a 20 nm chromium layer using a Quorum coater (Q150T ES Plus, East Sussex, UK) to enhance conductivity and minimize charging effects. SE images were acquired with a Tescan Solaris Field-Emission Scanning Electron Microscope (Brno, Czech Republic) under the following conditions: an accelerating voltage of 2–5 kV, beam current of 100–300 pA, and working distance of 5 mm, providing optimal spatial resolution. Hydrogel beads were not used for SEM analysis because their high water content is incompatible with the vacuum environment of the microscope.

2.14 Release study

Release studies were performed with 0.8 g of freeze-dried beads in 40 mL of distilled water at room temperature. The mixture was then stirred on a magnetic stirrer at defined time intervals (5, 10, 20, and 30 minutes). At each time point, 3 mL of the supernatant was collected for Folin and TMAC analysis. The amounts of TPC and TMAC in the samples were calculated as percentage values. The kinetic values were calculated as described by Dallabona *et al.* (2020)[20] using Microsoft Excel (Version 2021, Microsoft Corporation, Redmond, WA, USA).

2.15 Statistical analysis

All experiments were performed in triplicate ($n = 3$), and results are expressed as mean ± standard deviation. The coefficient of variation (CV) was maintained at ≤10% for all measurements. Data analysis was performed using IBM SPSS Statistics (Version 20.0, SPSS Inc., Chicago, IL, USA). Statistical differences among samples were determined using one-way analysis of variance (ANOVA), and Tukey's Honestly Significant Difference (HSD) test at a significance level of $p \leq 0.05$.

3 Results and discussion

3.1 Extract properties

Table 1 shows the content of phenolic acids, TPC, TMAC, and FRAP value of the aqueous SSCP extract. This phenolic extract was obtained using water as a green, food-grade solvent[25] *via* ultrasound-assisted extraction, yielding a substantial amount of phenolic compounds.[26] In our previous work, we showed that such extracts from SSCP are rich in anthocyanins and other flavonoids, with cyanidin 3-rutinoside, epicatechin, catechin, quercetin, kaempferol, naringenin, and cyanidin 3-glucoside, listed from the highest to the lowest concentration.[4] Table 1 complements the previous result, indicating that phenolic acids are also present in this extract. The high concentration of these compounds contributed to the extract's strong antioxidant capacity (521.29 ± 12.25 mg TE per L, as measured by the FRAP assay). These characteristics emphasize the potential of SSCP extract for food applications, either in its free form or as an encapsulated ingredient. For instance, extracts derived from sour cherry pomace after juice production have previously been encapsulated in whey and soy proteins for incorporation into cookies.[17] The present study builds on this concept by encapsulating SSCP extracts obtained from liqueur production, thereby establishing a foundation for future applications of this by-product as a functional food ingredient.

Table 1 Phenolic profile, and TPC, TMAC, and FRAP values of the extract[a]

Components	Values	CV (%)
Vanillic acid (mg L^{-1})	3.06 ± 0.18	5.88
Syringic acid (mg L^{-1})	0.94 ± 0.05	5.32
Chlorogenic acid (mg L^{-1})	13.37 ± 1.34	10.02
Caffeic acid (mg L^{-1})	3.04 ± 0.23	7.56
TPC (mg GAE per L)	249.11 ± 3.65	1.46
TMAC (mg L^{-1})	18.53 ± 0.23	1.24
FRAP (mg TE per L)	521.29 ± 12.25	2.35

[a] Results are reported as mean ± standard deviation ($n = 3$). The coefficient of variation (CV) for all results is approximately ≤10%.

3.2 Encapsulation efficiency (EE) and process yield

EE is known to vary depending on the concentration and physicochemical properties of the incorporated compounds and polymers, such as viscosity, pH, polarity, stability, *etc.*[27–30] In this study, the EE of Ca(II)-alginate beads formulated with different concentrations of inulin was evaluated based on the TPC and TMAC of SSCP extract and inulin content (Table 2). The EE of TPC was determined using two methods, considering the content of either loaded or unloaded compounds to highlight the differences and precision of these methods. Due to the alkaline pH of sodium citrate, which interferes with the pH-differentiation principle of the TMAC assay,[20] TMAC could not be measured based on the loaded compounds; therefore, it was measured based on the content of unloaded compounds found in the residual calcium chloride.

When EE for TPC was calculated from the loaded compounds in the beads, a significant increase was observed with increasing inulin concentration. However, when EE was determined from the unloaded compounds, the opposite trend emerged, with higher inulin levels reducing the encapsulation of phenolic compounds. This inconsistency likely arises from interference by inulin in the Folin-Ciocalteu assay when the content of loaded phenolic compounds is considered for EE calculation. Indeed, the inulin employed in the bead formulation exhibited a measurable TPC of 74.79 ± 2.28 μg GAE per g

Table 2 Encapsulation efficiency (EE) of extract components (TPC and TMAC) and inulin, as well as the encapsulation process yield in Ca(II)-alginate beads formulated with varying inulin concentrations[a]

Inulin level in the feed solution (% w/w)	EE (%) based on bead dissolution in sodium citrate solution	EE (%) based on unloaded compounds found in residual calcium chloride solution			
	TPC	TPC	TMAC	Inulin	Process yield (%)
0	54.17 ± 5.67^{a}	44.65 ± 0.49^{d}	47.18 ± 2.54^{ab}	—	81.00 ± 0.44^{a}
2.5	71.54 ± 1.21^{b}	39.40 ± 0.65^{c}	42.52 ± 1.09^{a}	97.06 ± 0.09^{e}	83.02 ± 0.28^{b}
5	78.07 ± 2.99^{b}	35.20 ± 0.57^{a}	42.85 ± 0.98^{a}	94.89 ± 0.04^{d}	85.62 ± 0.50^{c}
7.5	88.58 ± 4.16^{c}	37.47 ± 0.35^{b}	47.20 ± 1.48^{ab}	92.99 ± 0.04^{c}	86.07 ± 0.36^{c}
10	98.17 ± 1.98^{d}	37.31 ± 1.04^{b}	50.57 ± 3.50^{bc}	91.42 ± 0.13^{b}	90.27 ± 0.25^{d}
15	97.89 ± 1.06^{d}	36.07 ± 0.08^{ab}	53.26 ± 0.91^{c}	87.32 ± 0.08^{a}	93.33 ± 0.28^{e}

[a] Results are reported as mean ± standard deviation ($n = 3$). Different letters in each column show a significant difference ($p \leq 0.05$) among the samples, as assessed by one-way ANOVA and Tukey's Honestly Significant Difference (HSD) tests.

when analyzed independently. Since the majority of inulin is incorporated into the beads, as indicated by inulin-based EE values, its presence may artificially inflate the measured TPC of beads dissolved in sodium citrate, leading to an overestimation of the loaded phenolic compounds. Thus, in systems containing other reducing agents, such as inulin and its hydrolysis products, determination of TPC-based EE *via* bead dissolution in sodium citrate is not recommended, as it may yield misleading results.

This overestimation could be further exacerbated by the acidic environment of the feed solution, which promotes partial hydrolysis of inulin into reducing sugars (*e.g.,* fructose and D-glucose).[12] Indeed, the SSCP extract used in the present study had a notably acidic pH (3.59 ± 0.10), which may participate in the hydrolysis of inulin. Moreover, the inulin exhibited significant ferric-reducing capacity in the FRAP assay (97.46 ± 1.29 μg TE per g), further supporting its reducing potential and contribution to overestimated TPC readings. Therefore, based on EE calculations derived from the quantification of unloaded compounds remaining in the calcium chloride solution, it can be inferred that the addition of inulin actually reduces the TPC-based EE in Ca(II)-alginate beads. This effect is likely due to competitive interactions between inulin and phenolic compounds, with inulin occupying a greater proportion of the bead matrix and consequently limiting the incorporation of bioactive molecules.

Table 3 summarizes previous studies on the encapsulation of phenolic extracts using calcium alginate and inulin. As shown, all those studies dissolved the beads in sodium citrate to measure TPC for EE estimation, and they mostly reported that inulin increased the EE of TPC. However, such increases are likely overestimated due to the interference of inulin and its monomers with the Folin–Ciocalteu assay. Future studies are therefore advised to quantify EE based on the unloaded compounds or, preferably, to determine individual phenolic compounds using chromatographic techniques for more reliable results. For example, Li *et al.* (2021)[14] analyzed individual phenolic compounds in Ca(II)-alginate-inulin beads using HPLC and found that the EE of certain compounds increased, whereas others decreased or remained unchanged.

On the other hand, the beads with the highest inulin concentration exhibited the highest TMAC-based EE. Anthocyanins, which represent a specific subclass of phenolic compounds, may be preferentially stabilized by inulin; thus, their EE increased with higher inulin content. This trend suggests that elevated inulin concentrations enhance the entrapment of anthocyanins within the bead matrix, likely due to favorable hydrogen bonding or other molecular interactions between inulin and anthocyanins. A plausible explanation for this effect lies in the polarity of anthocyanins, which are highly hydrophilic and structurally suited to interact with hydrophilic carriers such as inulin.[33] These interactions may help reduce anthocyanin diffusion from the matrix during gelation, thereby improving retention and stability. However, due to their hydrophilic nature, some anthocyanins may still leach into the $CaCl_2$ cross-linking solution during bead formation, resulting in a reduction of EE.[11]

Moreover, inulin incorporation markedly improved the process yield, which is likely attributable to the increased solid content of the feed solution. The overall results in this section revealed that the formulation of inulin-enriched matrices should be optimized to balance the EE of TMAC and TPC with the prevention of leaching during encapsulation. Moreover, pretreating the feed solution before the encapsulation process may significantly enhance the loading of different compounds into the beads. For instance, recent studies have reported that ultrasound treatment can promote the formation of inulin-polyphenol complexes, which enhance the antioxidant activity and stability of polyphenols and expand their potential applications in food systems.[34] Therefore, applying ultrasound-assisted complexation prior to encapsulation could be a promising strategy to improve the interaction between inulin and phenolic compounds, potentially increasing EE, and the functional performance of the resulting beads.

3.3 Physicochemical properties of the beads

The physical properties of the beads play a key role in determining their texture, structure, and potential performance. Table 4 presents the physical properties of the hydrogel beads immediately after preparation, including texture profile

Table 3 Previous studies on the encapsulation of phenolic extracts using inulin and sodium alginate

Phenolic extract	Sodium alginate concentration (%)	Feed solution preparation	EE determination method	EE	References
Amazonian berry extracts	1.5	Sodium alginate and inulin solutions were prepared directly in the extract	EE measured after bead dissolution in sodium citrate; antioxidant activity (ABTS) compared before and after encapsulation	EE without inulin: 89.1 ± 1% EE with 2.5% inulin: 94.7 ± 2%	Moreira Mar *et al.* (2021)[11]
Chokeberry (*Aronia melanocarpa* L.) extract	1.5	Sodium alginate and inulin solutions were prepared directly in the extract	EE measured after bead dissolution in sodium citrate; TPC compared before and after encapsulation	They reported an increase in the TPC of the beads after adding 5% *w/v* inulin	Ćujić *et al.* (2016)[13]
Carqueja extract	1.5	The extract at 2 mg mL^{-1} was added to a 1.5% sodium alginate solution, and then inulin was mixed	EE measured after bead dissolution in sodium citrate; TPC compared before and after encapsulation	EE without inulin: 49.0 ± 3.1% EE with 20% inulin: 73.8 ± 2.8%	Balanč *et al.* (2015)[31]
Thyme (*Thymus serpyllum* L.) aqueous extract	1.5	Sodium alginate and inulin solutions were prepared directly in the extract	EE measured after bead dissolution in sodium citrate; TPC compared before and after encapsulation	EE without inulin: 51 ± 3% EE with 5% inulin: 79 ± 5%	Stojanovic *et al.* (2012)[32]
Tea polyphenols	2	Sodium alginate and inulin solution were added separately to 3 mg mL^{-1} tea polyphenol solution and then mixed in a proportion of 80 : 20 (*w/w*)	EE measured after bead dissolution in sodium citrate; TPC compared before and after encapsulation	EE without inulin: 38.51 ± 1.96 EE with 2% inulin: 36.48 ± 1.57	Li *et al.* (2021)[14]

Table 4 Mechanical properties of Ca(II)-alginate hydrogel beads formulated with varying inulin concentrations[a]

	Inulin concentration (% w/w)					
Parameter	0	2.5	5	7.5	10	15
Hardness	11.20 ± 2.01^{b}	9.39 ± 0.37^{ab}	6.70 ± 0.26^{a}	8.48 ± 0.49^{ab}	7.07 ± 1.48^{a}	8.23 ± 1.02^{ab}
Springiness	2.41 ± 1.07^{a}	3.48 ± 0.65^{a}	2.41 ± 0.23^{a}	2.67 ± 0.27^{a}	2.77 ± 0.31^{a}	2.74 ± 0.90^{a}
Cohesiveness	0.54 ± 0.01^{a}	0.51 ± 0.02^{a}	0.52 ± 0.05^{a}	0.48 ± 0.05^{a}	0.51 ± 0.01^{a}	0.49 ± 0.02^{a}
Elasticity index	0.58 ± 0.19^{a}	0.43 ± 0.04^{a}	0.56 ± 0.03^{a}	0.49 ± 0.05^{a}	0.52 ± 0.01^{a}	0.53 ± 0.12^{a}
Gumminess	6.02 ± 1.23^{b}	4.77 ± 0.20^{ab}	3.46 ± 0.19^{a}	4.06 ± 0.23^{a}	3.62 ± 0.82^{a}	4.03 ± 0.45^{a}
Resilience	0.79 ± 0.05^{a}	0.78 ± 0.04^{a}	0.72 ± 0.03^{a}	0.69 ± 0.05^{a}	0.74 ± 0.05^{a}	0.78 ± 0.02^{a}
Diameter (mm)	3.47 ± 0.27^{a}	3.92 ± 0.13^{ab}	4.41 ± 0.29^{bc}	4.34 ± 0.14^{c}	4.62 ± 0.19^{c}	4.68 ± 0.12^{c}

[a] Results are reported as mean ± standard deviation ($n = 3$). Different characters in each row show a significant difference ($p \leq 0.05$) among the samples, as assessed by one-way ANOVA and Tukey's honestly significant difference tests.

analyzer parameters and bead diameter. Beads without inulin exhibited significantly higher hardness and gumminess values ($p \leq 0.05$). Similarly, Li *et al.* (2021) reported that the addition of inulin to Ca(II)-alginate beads loaded with tea polyphenols significantly reduced the hardness of hydrogel beads.[14] Moreover, Balanč *et al.* (2016) reported that the addition of inulin to the alginate matrix leads to a softer structure. They reported that the incorporation of inulin may decrease the cross-linking density, yielding softer structures.[31] This can be attributed to the increase in the viscosity of the feed solution due to the addition of inulin (Fig. 2a and b), which likely restricts calcium ion diffusion during cross-linking, resulting in a less compact gel structure and reduced mechanical integrity.[35] Therefore, optimizing the concentrations of both wall materials and the cross-linking agent in the gelling solution is essential to obtain beads with improved physical properties.

However, the inclusion of inulin in the feed solution led to a noticeable increase in the diameter of the hydrogel beads (Table 4), and this trend persisted even after freeze-drying (Fig. 3). This enlargement could be attributed to the higher

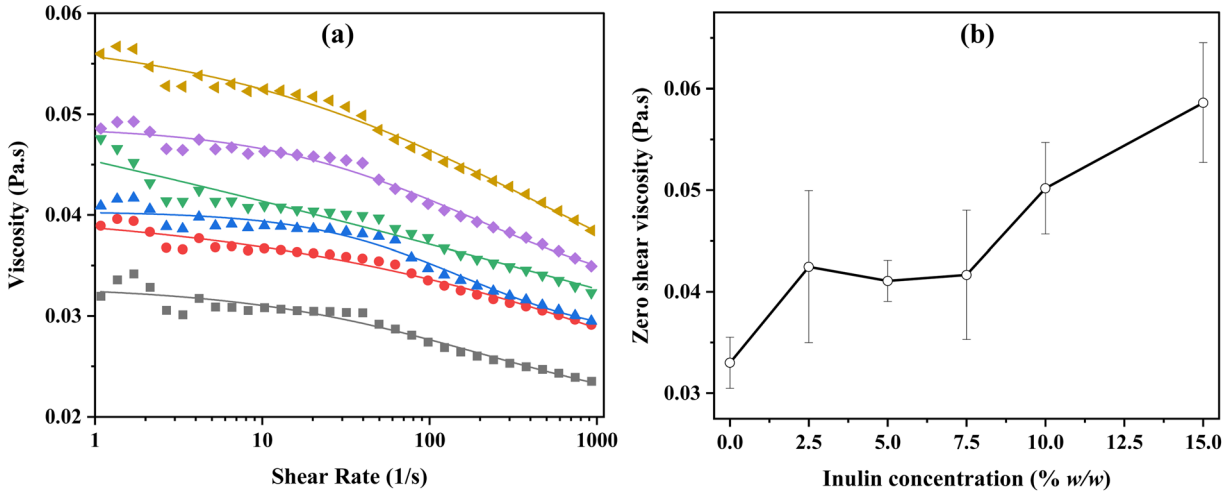

Fig. 2 (a) Viscosity (η) as a function of shear rate (γ) for feed solutions containing inulin at concentrations of 0 (□, $R^2 = 0.943$), 2.5 (●, $R^2 = 0.968$), 5 (▲, $R^2 = 0.966$), 7.5 (▼, $R^2 = 0.938$), 10 (♦, $R^2 = 0.981$), and 15 (▶, $R^2 = 0.982$) % w/w, fitted using the cross model. (b) Zero-shear viscosity (η_0) as a function of inulin concentration in the feed solutions. Data points show mean ± SD ($n = 3$).

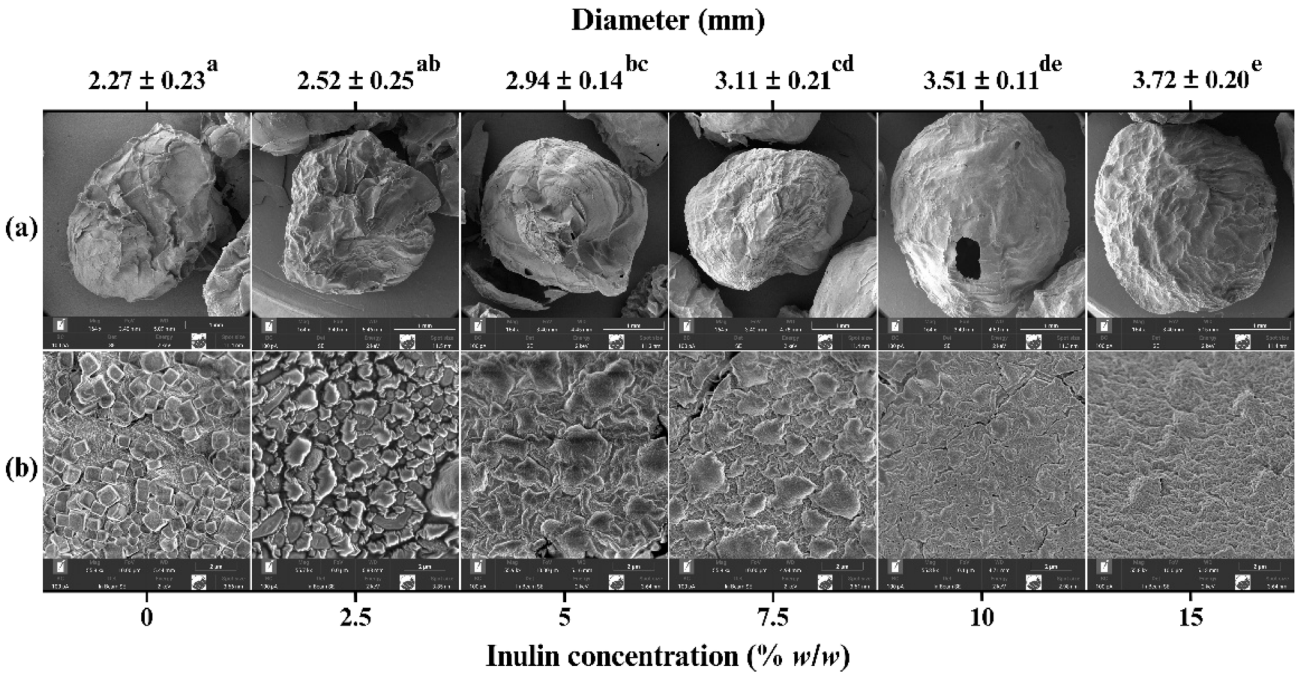

Fig. 3 Secondary electron microscopy (SEM) images and the diameter of the freeze-dried beads with varying inulin concentrations. (a) Particle morphology at 164× magnification (Field of view: 3.40 mm). (b) Surface morphology at 56000× magnification (Field of view: 10 μm). Different letters denoting dimeter values show a significant difference ($p \leq 0.05$) among the samples, as assessed by one-way ANOVA and Tukey's Honestly Significant Difference (HSD) tests.

viscosity and reduced surface tension of the inulin-alginate mixture (*i.e.,* the feed solution), which may lead to larger beads. As shown in Fig. 2(a and b), the viscosity of the feed solutions increased significantly with inulin addition ($p \leq 0.05$), reaching its maximum at the highest inulin concentration.

Moreover, the combination of sodium alginate with other materials can fill pores and impact the bead size.[11] Particularly, the filling capacity of inulin in Ca(II)-alginate has been proven in previous studies.[36] Similarly to our findings, Moreira Mar *et al.* (2021) showed that increasing the inulin concentration can contribute to an increase in the diameter of beads. Fig. 3 shows the secondary electron microscopy (SEM) images and diameter of the freeze-dried beads with varying inulin concentrations (0–15%) at low (a) and high (b) magnification. The images clearly show that when inulin is added at higher concentrations, it occupies space within the gel matrix of Ca(II)-alginate, thereby contributing to a bigger diameter of the beads.

Table 5 Moisture content, water activity, and hygroscopicity of the hydrogel and freeze-dried beads prepared with different inulin concentrations[a]

	Moisture content (%)		Water activity		Hygroscopicity (%)
Inulin concentration (% w/w)	Hydrogel beads	Freeze-dried beads	Hydrogel beads	Freeze-dried beads	Freeze-dried beads
0	94.07 ± 0.15^{d}	5.97 ± 0.34^{a}	0.909 ± 0.002^{a}	0.160 ± 0.002^{d}	4.98 ± 0.26^{c}
2.5	93.65 ± 0.51^{cd}	8.05 ± 1.61^{a}	0.909 ± 0.003^{a}	0.143 ± 0.002^{c}	5.32 ± 0.11^{c}
5	93.43 ± 0.12^{bc}	8.24 ± 0.59^{a}	0.911 ± 0.004^{a}	0.136 ± 0.002^{b}	4.71 ± 0.06^{bc}
7.5	92.84 ± 0.13^{b}	8.69 ± 0.42^{a}	0.912 ± 0.004^{a}	0.135 ± 0.002^{ab}	4.02 ± 0.17^{ab}
10	91.11 ± 0.07^{a}	7.94 ± 1.09^{a}	0.911 ± 0.002^{a}	0.130 ± 0.001^{a}	3.43 ± 0.11^{a}
15	91.61 ± 0.08^{a}	8.51 ± 1.35^{a}	0.911 ± 0.001^{a}	0.131 ± 0.003^{ab}	3.26 ± 0.32^{a}

[a] Results are reported as mean ± standard deviation ($n = 3$). Different letters in each column show a significant difference ($p \leq 0.05$) among the samples, as assessed by one-way ANOVA and Tukey's Honestly Significant Difference (HSD) tests.

Overall, the effect of inulin on the physical properties of the feed solution and the beads may be responsible for the lower EE of the extract in the beads. While inulin increased the viscosity of the feed solution (Fig. 2a and b), which could limit phenolic diffusion during droplet formation, it may simultaneously act as a non-gelling polysaccharide within the Ca(II)-alginate network. As reported by Toprakçı *et al.* (2022),[37] an increase in feed solution viscosity can lead to greater occupation of internal bead volume by the wall material, ultimately resulting in lower EE due to reduced space available for the active compounds. Consequently, inulin incorporation increases internal volume occupancy in the beads (Fig. 3) without contributing to network formation, yielding softer beads (Table 4) with diminished entrapment capacity. This softening, together with competitive space occupancy by inulin, facilitates phenolic leakage into the external medium during gelation, leading to higher phenolic content in the unloaded fraction and lower EE. Therefore, the denser alginate structure formed without inulin may better trap the active compounds, preventing their loss during preparation or handling. However, adding inulin to the beads is preferred as it may enhance the functional properties of the beads, such as their prebiotic activity and potential health benefits, making them more suitable for targeted use in food or pharmaceutical formulations. Therefore, Ca(II)-alginate beads without inulin and those containing 2.5% (w/w) inulin were selected for the next step of the project to study the release of bioactive compounds.

To conduct the release study in the subsequent stage, a drying step was applied to improve the physical properties of the beads, as dried microbeads generally exhibit greater stability and mechanical strength compared to their hydrogel counterparts. In addition, drying helps to prevent microbial growth during storage. However, dehydration during the drying process can disrupt the structural integrity of the Ca(II)-alginate matrix, resulting in reduced bead sphericity. To mitigate this issue, some researchers have proposed incorporating inulin as a filler.[13] Table 5 presents the moisture content, water activity, and hygroscopicity of the hydrogel and freeze-dried beads prepared with varying inulin concentrations. Drying significantly reduced both the moisture content and water activity across all formulations. Notably, beads containing inulin exhibited significantly lower water activity after drying, which is advantageous for storage stability. Since hydrogel beads showed no hygroscopic behavior, hygroscopicity results are reported only for the freeze-dried samples. Similarly, Moreira Mar *et al.* (2021)[11] reported a reduction in bead moisture following the incorporation of inulin into the bead formulation.

3.4 Release kinetics of TMAC and TPC from the beads

The release behavior of bioactive compounds from encapsulated systems significantly influences their stability and functional performance in targeted food applications. The release profiles of TPC and TMAC from the bead formulations with inulin (2.5% w/w) and without inulin over 30 minutes are presented in Fig. 4. For both compounds, the inulin-free beads demonstrated greater polyphenol retention during the initial rapid release phase within the first 5 minutes, while the inulin-containing beads exhibited enhanced release during the plateau phase. This initial release phase is frequently associated with low molecular weight compounds and is primarily attributed to their partial retention or preferential localization near or on the surface of the polymeric matrix during the formulation process.[38] Lyophilization may further support the enhanced initial release, as the migration of water toward the surface during dehydration could facilitate the rapid liberation of compounds in the early stages.[39] Similar findings were reported by Arriola *et al.* (2016)[1] where stevia aqueous extract-loaded wet beads released ~50% of polyphenols within the first 10 minutes, while lyophilized beads reached ~55%. Following this initial rapid release, our results demonstrated a plateau phase, suggesting a transition to a more prolonged and controlled release of the encapsulated compounds from the bead matrix, which could be attributed to the release of the encapsulated bioactive compound from the core of the microcapsules.

In the present study, the inulin-containing beads exhibited a higher release of both TPC and TMAC compared to the plain Ca(II)-alginate beads. During the rapid release phase, beads with inulin released 67.16 ± 2.46% of TPC and 54.48 ± 0.66% of TMAC, whereas the inulin-free beads showed lower release rates, with 54.98 ± 0.78% for TPC and 49.28 ± 0.17% for TMAC. This difference in release behavior suggests that inulin may significantly influence the matrix structure and interactions

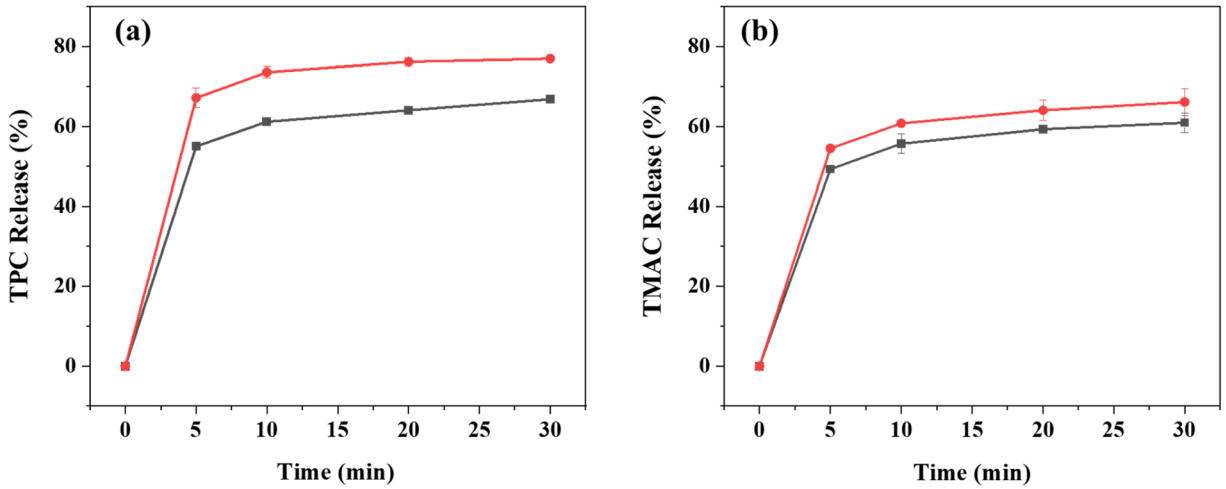

Fig. 4 Release profiles of (a) TPC and (b) TMAC from freeze-dried beads without (■) and with (●) inulin (2.5% w/w) over 30 minutes.

Table 6 Release kinetics parameters of TPC and TMAC from bead formulations with and without inulin fitted to five kinetic models[a]

		TPC			TMAC		
Models	Inulin concentration (% w/w)	n	k	R^2	n	k	R^2
Zero-order	0	—	0.428	0.878	—	0.428	0.842
	2.5	—	0.347	0.753	—	0.424	0.857
First order	0	—	0.005	0.906	—	0.004	0.866
	2.5	—	0.005	0.786	—	0.005	0.885
Korsmeyer–Peppas	0	0.105	47.054	0.968	0.117	41.650	0.958
	2.5	0.075	60.190	0.910	0.106	46.420	0.964
Higuchi	0	—	3.433	0.935	—	3.460	0.914
	2.5	—	2.852	0.841	—	3.419	0.923
Hixson–Crowell	0	—	0.013	0.897	—	0.011	0.858
	2.5	—	0.013	0.775	—	0.012	0.876

[a] Note: k values are not comparable across models and are model-specific; R^2 is used to assess the best fit. n: release exponent, k: release rate constant, and R^2: coefficient of determination.

between compounds. Consistent with our findings, in a study in which chokeberry extract was encapsulated in Ca(II)-alginate-inulin beads, significantly higher phenolic release was observed from freeze-dried sodium alginate beads containing inulin than from those without inulin.[13] However, other studies also reported a decrease in the release rate when inulin was added to alginate-inulin beads.[11,31] These contradictions may be related to the bead formulation, the type and source of inulin used, the polymer's physicochemical properties, or the pH and phenolic profile of the extract, all of which may lead to distinct release behaviors.

The release mechanisms were investigated by fitting the experimental data into five different kinetic models: zero-order, first-order, Korsmeyer–Peppas, Higuchi, and Hixson–Crowell (Table 6). The release kinetics of TPC and TMAC from bead formulations, with and without inulin, were best described by the Korsmeyer–Peppas model, as evidenced by the highest determination coefficients (R^2 = 0.968 for TPC and 0.964 for TMAC). This indicates that the release mechanism is primarily diffusion-driven, as evidenced by n values below 0.5, consistent with Fickian diffusion. The Higuchi model also exhibited a good fit for both compounds (R^2 > 0.91), reinforcing the predominance of diffusion-controlled release from the matrix. Conversely, zero-order and first-order models showed lower R^2 values, particularly for TPC with inulin, indicating that constant-rate or concentration-dependent release may not fully describe the system. The Hixson–Crowell model provided a moderate fit, suggesting a limited contribution of surface-area changes to the release process.

4 Conclusion

This study sought to clarify the actual role of inulin as a co-carrier in Ca(II)-alginate encapsulation of phenolic extracts, with particular emphasis on EE, bead physical properties, and release behavior. The results demonstrate that inulin exhibits a dual and method-dependent effect on encapsulation performance. When encapsulation efficiency was determined by bead

dissolution in sodium citrate, the addition of inulin significantly increased TPC-based EE, an effect attributable to inulin's intrinsic reducing capacity, which interferences with the Folin-Ciocalteu assay. In contrast, when this analytical interference was eliminated by calculating EE based on unloaded compounds found in the cross-linking medium, TPC-based EE decreased with increasing inulin concentration. These findings highlight the critical importance of selecting appropriate EE determination methods when evaluating systems containing reducing polysaccharides.

In parallel, inulin significantly influenced the physical characteristics of the beads, producing larger, softer Ca(II)-alginate particles. These structural changes were associated with enhanced diffusion-controlled release, characterized by a more pronounced release during the later phase and higher overall release of both phenolics and anthocyanins. Despite a reduction in apparent TPC-based EE when interference-free calculations were applied, inulin enhanced anthocyanin-based EE, underscoring its selective benefit across bioactive compound classes.

This research addressed the limitations of spectrophotometric assays for measuring EE, which are susceptible to pH changes and interference from reducing agents, such as inulin. While chromatographic methods can provide more precise quantification, the proposed approach based on unloaded compounds offers a rapid, cost-effective alternative. Moreover, the use of the residual cross-linking solution enables the assessment of anthocyanin-based EE through spectrophotometric methods that cannot be applied to bead-dissolution approaches due to pH changes. Future studies should focus on optimizing formulation parameters, such as inulin molecular weight, concentration, and alginate-to-calcium ratios, and on integrating chromatographic assays to further elucidate encapsulation mechanisms. Overall, despite the dual effects of inulin, employing it as a dietary fiber co-carrier remains promising for clean-label encapsulation systems, provided that formulation and analytical strategies are carefully optimized.

Author contributions

Peyman Ebrahimi: conceptualization, data curation, formal analysis, investigation, methodology, software, supervision, validation, visualization, writing – original draft, writing – review & editing. Alberto De Iseppi: investigation, data curation. Zeynep Gülbeş: investigation, visualization. Elisa Canazza: investigation. Jacopo Nava: investigation. Barbara Simonato: resources, data curation, validation. Corrado Rizzi: resources, data curation, validation. Dasha Mihaylova: resources, data curation, validation. Anna Lante: conceptualization, data curation, formal analysis, methodology, project administration, resources, supervision, validation.

Conflicts of interest

There are no conflicts to declare.

Data availability

All the data are presented in the article. Additional information will be provided upon request.

Acknowledgements

This research was funded through grant agreement number CUP J15B24001760008. The authors acknowledge the help of Luciano Magro in performing some of the analysis.

References

1 N. D. Aceval Arriola, P. M. de Medeiros, E. S. Prudencio, C. M. Olivera Müller and R. D. de Mello Castanho Amboni, *Food Biosci.*, 2016, **13**, 32–40, DOI: 10.1016/j.fbio.2015.12.001.
2 G. S. da Rosa, T. R. Martiny, G. L. Dotto, S. K. Vanga, D. Parrine, Y. Gariepy, M. Lefsrud and V. Raghavan, *Sustain. Mater. Technol.*, 2021, **28**, e00276, DOI: 10.1016/j.susmat.2021.e00276.
3 A. Manthei, P. Elez-Martínez, O. Martín-Belloso and R. Soliva-Fortuny, *Sustain. Food Technol.*, 2024, **2**(6), 1757–1769, DOI: 10.1039/D4FB00215F.
4 P. Ebrahimi, A. Roodbali, B. Simonato, A. Lante and C. Rizzi, *Ultrason. Sonochem.*, 2025, **118**, 107375, DOI: 10.1016/j.ultsonch.2025.107375.
5 S. Ghosh, T. Sarkar, A. Das and R. Chakraborty, *LWT*, 2022, **153**, 112527, DOI: 10.1016/j.lwt.2021.112527.
6 P. B. Rahul, R. K. Tiwari, K. K. Dash and M. Sharma, *Sustain. Food Technol.*, 2024, **3**(1), 123–144, DOI: 10.1039/D4FB00196F.
7 E. Akpo, C. Colin, A. Perrin, J. Cambedouzou and D. Cornu, *Materials*, 2024, **17**(11), 2774, DOI: 10.3390/ma17112774.
8 Y. Song, L. Liu, H. Shen, J. You and Y. Luo, *Food Control*, 2011, **22**(3–4), 608–615, DOI: 10.1016/j.foodcont.2010.10.012.
9 Z. Khoshdouni Farahani, M. Mousavi, M. Seyedain Ardebili and H. Bakhoda, *Food Chem. Adv.*, 2023, **2**, 100195, DOI: 10.1016/j.focha.2023.100195.
10 P. Yan, W. Lan and J. Xie, *Trends Food Sci. Technol.*, 2024, **143**, 104217, DOI: 10.1016/j.tifs.2023.104217.
11 J. Moreira Mar, L. Souza da Silva, M. da S. Rabello, M. Moraes Biondo, V. Ferreira Kinupp, P. Henrique Campelo, E. Bruginski, F. Ramos Campos, J. de Araújo Bezerra and E. Aparecido Sanches, *Food Res. Int.*, 2021, **139**, 109838, DOI: 10.1016/j.foodres.2020.109838.
12 E. Canazza, M. Grauso, D. Mihaylova and A. Lante, *Gels*, 2025, **11**(10), 829, DOI: 10.3390/gels11100829.
13 N. Ćujić, K. Trifković, B. Bugarski, S. Ibrić, D. Pljevljakušić and K. Šavikin, *Ind. Crops Prod.*, 2016, **86**, 120–131, DOI: 10.1016/j.indcrop.2016.03.045.
14 Q. Li, M. Duan, D. Hou, X. Chen, J. Shi and W. Zhou, *Food Hydrocoll.*, 2021, **112**, 106274, DOI: 10.1016/j.foodhyd.2020.106274.
15 D. Turck, T. Bohn, M. de la Montaña Cámara Hurtado, J. Castenmiller, S. De Henauw, Á. Jos, A. Maciuk,

I. Mangelsdorf, B. Mcnulty, A. Naska, K. Pentieva, A. Siani, F. Thies, M. Aguilera Gómez, T. Frenzel, H. J. McArdle, P. Moldeus, M. Neuhäuser-Berthold, J. R. Schlatter, H. van Loveren, L. Matijević and K. I. Hirsch-Ernst, *EFSA J*, 2025, **23**(7), e9534, DOI: 10.2903/j.efsa.2025.9534.

16 S. K. Pournaki, R. S. Aleman, M. Hasani-Azhdari, J. Marcia, A. Yadav and M. Moncada, *J: Multidiscip. Sci. J.*, 2024, **7**(3), 281–301, DOI: 10.3390/j7030016.

17 V. Tumbas Šaponjac, G. Ćetković, J. Čanadanović-Brunet, B. Pajin, S. Djilas, J. Petrović, I. Lončarević, S. Stajčić and J. Vulić, *Food Chem.*, 2016, **207**, 27–33, DOI: 10.1016/j.foodchem.2016.03.082.

18 A. M. Oancea, M. Hasan, A. M. Vasile, V. Barbu, E. Enachi, G. Bahrim, G. Râpeanu, S. Silvi and N. Stănciuc, *LWT*, 2018, **95**, 129–134, DOI: 10.1016/j.lwt.2018.04.083.

19 P. Ebrahimi, L. Hoxha, D. Mihaylova, M. Nicoletto and A. Lante, *J. Sci. Food Agric.*, 2024, **104**(15), 9559–9568, DOI: 10.1002/jsfa.13780.

20 I. Dalponte Dallabona, G. G. de Lima, B. I. Cestaro, I. de S. Tasso, T. S. Paiva, E. J. G. Laureanti, L. M. de M. Jorge, B. J. G. da Silva, C. V. Helm, A. L. Mathias and R. M. M. Jorge, *Int. J. Biol. Macromol.*, 2020, **163**, 1421–1432, DOI: 10.1016/j.ijbiomac.2020.07.256.

21 N. Teslić, A. Curioni, M. Marangon, A. Stupar, G. Lomolino, H. Jones-Moore and A. De Iseppi, *Food Chem.*, 2025, **493**, 145742, DOI: 10.1016/j.foodchem.2025.145742.

22 K. Azuma, K. Ippoushi, H. Ito, H. Higashio and J. Terao, *J. Sci. Food Agric.*, 1999, **79**(14), 2010–2016.

23 L. Zhou, X. Guo, J. Bi, J. Yi, Q. Chen, X. Wu and M. Zhou, *J. Food Process. Preserv.*, 2017, **41**(1), 1–11, DOI: 10.1111/jfpp.12734.

24 M. Pattnaik and H. N. Mishra, *J. Food Process. Preserv.*, 2020, **44**(4), 1–15, DOI: 10.1111/jfpp.14374.

25 D. Mihaylova and A. Lante, *Open Biotechnol. J.*, 2019, **13**(1), 155–162, DOI: 10.2174/1874070701913010155.

26 D. Ağagündüz, G. Ayakdaş, B. Katırcıoğlu and F. Ozogul, *Sustain. Food Technol.*, 2025, **3**(5), 1284–1308, DOI: 10.1039/D5FB00136F.

27 K. Singh, B. Adhikari, J. Low, M. A. Brennan, L. Newman, C. S. Brennan and N. Utama-ang, *Sci. Rep.*, 2023, **13**(1), 1–16, DOI: 10.1038/s41598-023-46339-x.

28 A. M. Naranjo-Durán, J. Quintero-Quiroz, J. Rojas-Camargo and G. L. Ciro-Gómez, *Sci. Rep.*, 2021, **11**(1), 1–10, DOI: 10.1038/s41598-020-80119-1.

29 S. Kanokpanont, R. Yamdech and P. Aramwit, *Artif. Cells, Nanomedicine Biotechnol.*, 2018, **46**(4), 773–782, DOI: 10.1080/21691401.2017.1339050.

30 A. Gomes, A. L. R. Costa, L. H. Fasolin and E. K. Silva, *Carbohydr. Polym.*, 2025, **347**, 122742, DOI: 10.1016/j.carbpol.2024.122742.

31 B. Balanč, A. Kalušević, I. Drvenica, M. T. Coelho, V. Djordjević, V. D. Alves, I. Sousa, M. Moldão-Martins, V. Rakić, V. Nedović and B. Bugarski, *J. Food Sci.*, 2016, **81**(1), E65–E75, DOI: 10.1111/1750-3841.13167.

32 R. Stojanovic, A. Belscak-Cvitanovic, V. Manojlovic, D. Komes, V. Nedovic and B. Bugarski, *J. Sci. Food Agric.*, 2012, **92**(3), 685–696, DOI: 10.1002/jsfa.4632.

33 W. Fu, S. Li, H. Helmick, B. R. Hamaker, J. L. Kokini and L. Reddivari, *Foods*, 2023, **12**(9), 1846, DOI: 10.3390/foods12091846.

34 S. Li, D. Lei, Z. Zhu, J. Cai, M. Manzoli, L. Jicsinszky, G. Grillo and G. Cravotto, *Ultrason. Sonochem.*, 2021, **74**(68), 105568, DOI: 10.1016/j.ultsonch.2021.105568.

35 E. S. Chan, B. B. Lee, P. Ravindra and D. Poncelet, *J. Colloid Interface Sci.*, 2009, **338**(1), 63–72, DOI: 10.1016/j.jcis.2009.05.027.

36 S. Liu, Z. Fang and K. Ng, *Food Res. Int.*, 2022, **160**, 111749, DOI: 10.1016/j.foodres.2022.111749.

37 İ. Toprakçı, M. Torun and S. Şahin, *Foods*, 2022, **12**(1), 130, DOI: 10.3390/foods12010130.

38 X. Huang and C. S. Brazel, *J. Control. Release*, 2001, **73**(2–3), 121–136, DOI: 10.1016/S0168-3659(01)00248-6.

39 T. H. Kim and T. G. Park, *Int. J. Pharm.*, 2004, **271**(1–2), 207–214, DOI: 10.1016/j.ijpharm.2003.11.021.